Search for direct CP violation in charged charmless $B \to PV$ decays

R. Aaij *et al.*[*]
(LHCb Collaboration)

Measurements of CP asymmetry in charmless $B \to PV$ decays are presented, where P and V denote a pseudoscalar and a vector meson, respectively. Five different $B \to PV$ decays from four final states, $B^{\pm} \to \pi^{\pm}\pi^{+}\pi^{-}$, $B^{\pm} \to K^{\pm}\pi^{+}\pi^{-}$, $B^{\pm} \to K^{\pm}K^{+}K^{-}$ and $B^{\pm} \to \pi^{\pm}K^{+}K^{-}$ are analyzed. The measurements are based on a method that does not require full amplitude analyses, and are performed using proton-proton collision data at a center-of-mass energy of 13 TeV collected by LHCb between 2015 and 2018, corresponding to an integrated luminosity of 5.9 fb^{-1}. In the $\pi^{+}\pi^{-}$ P-wave, in the region dominated by the $B^{\pm} \to \rho(770)^{0}K^{\pm}$ decay, a CP asymmetry of $A_{CP} = +0.150 \pm 0.019 \pm 0.011$ is measured, where the first uncertainty is statistical and the second is systematic. This is the first observation of CP violation in this process. For the other four decay channels, in regions dominated by the $B^{\pm} \to \rho(770)^{0}\pi^{\pm}$, $B^{\pm} \to \overset{(-)}{K}{}^{*}(892)^{0}\pi^{\pm}$, $B^{\pm} \to \overset{(-)}{K}{}^{*}(892)^{0}K^{\pm}$ and $B^{\pm} \to \phi(1020)K^{\pm}$ decays, CP asymmetries in the P-wave compatible with zero are measured.

I. INTRODUCTION

In recent years, the large datasets produced at the LHC have allowed precise measurements of direct CP violation in B meson decays [1]. However, there are still a number of decay channels without precise CP -asymmetry measurements. Large samples of specific decays are required to improve our knowledge of CP asymmetries in charmless decays of B mesons, including those with neutral mesons in the final state. The start of Belle II [2] operations, the coming data-taking with an upgraded LHCb detector [3], and the analyses of the data already collected by the LHCb detector will allow the necessary measurements in the near future.

Theoretical developments using different approaches have resulted in many predictions for CP asymmetries. Many of these studies are focused on charmless two-body and quasi-two-body B -meson decays, in particular those to two pseudoscalar mesons ($B \to PP$) and to a pseudoscalar and a vector meson ($B \to PV$) [4–14]. These studies are directly linked to the long-standing controversy about the role of the short- and long-distance contributions to the generation of the strong-phase differences needed for direct CP violation to occur [1].

In this paper quasi-two-body $B \to PV$ decays, which result in three-body final states due to V decays, are studied. Given the large phase space of these B-meson decays, different types of resonant contributions are allowed. Therefore, in three-body final states the vector resonances interfere with other resonant components. The interference has been used to estimate the strong phases, as well as the contribution from penguin amplitudes [15–17]. Furthermore, the three-body environment can affect the amount of the CP violation associated with the $B \to PV$ decay amplitude [12].

The resonant structure of three-body decays can be studied with model-dependent amplitude analyses, a complex task given the large number of possible intermediate states. Recently, the LHCb Collaboration presented three CP -asymmetry measurements of $B \to PV$ decays based on a full Dalitz plot analysis of data collected in 2011 and 2012 [18–21]. From the amplitude analysis of the $B^{0} \to K_{S}^{0}\pi^{+}\pi^{-}$ decay, the CP asymmetry in the $B^{0} \to K^{*}(892)^{+}\pi^{-}$ decay was measured to be $A_{CP} = -0.308 \pm 0.062$ [18]. The A_{CP} measurement of the decay $B^{\pm} \to \overset{(-)}{K}{}^{*}(892)^{0}K^{\pm}$ from $B^{\pm} \to K^{\pm}\pi^{\mp}K^{\pm}$ decay was $0.123 \pm 0.087 \pm 0.045$ [19]. Finally, from the analysis of the $B^{-} \to \pi^{-}\pi^{+}\pi^{-}$ decay, the CP asymmetry of $B^{-} \to \pi^{-}\rho(770)^{0}$ decay was found to be consistent with zero, $A_{CP} = 0.007 \pm 0.019$ [20,21]. In the same analysis, CP asymmetries were observed in the $B^{-} \to \pi^{-}\sigma$ and $B^{-} \to \pi^{-}f_{2}(1270)$ decays, $A_{CP} = 0.160 \pm 0.028$ and $A_{CP} = 0.468 \pm 0.077$, respectively.

In this paper, measurements of CP asymmetries in charmless $B \to PV$ decays are presented. The measurements are based on data collected by the LHCb detector between 2015 and 2018, corresponding to 5.9 fb^{-1} of proton-proton (pp) collisions at a center-of-mass energy of 13 TeV. A new method [12] that does not rely on a full amplitude analysis is used. The method is based on three key features of three-body B decays: the large phase space; the dominance of scalar and vector resonances with masses below or around 1 GeV/c^2, confirmed by amplitude analyses performed by Belle [22,23], *BABAR* [24–27] and LHCb Collaborations [19–21]; and the clear signatures of the resonant amplitudes in the Dalitz plot. The method used in this analysis is suited for measuring the CP asymmetry between the yields of the $B^+ \to P^+V$ and $B^- \to P^-V$ decays.

In the decay $B^\pm \to R(\to h_1^- h_2^+) h_3^\pm$, where R is a resonance, the notation $s_\parallel$ is used for the two-body invariant mass squared $m^2(h_1^- h_2^+)$ and $s_\perp$ for $m^2(h_1^- h_3^+)$. The resonance line shape (typically a Breit-Wigner distribution) is observed in the projection of the Dalitz plot onto the $s_\parallel$ axis. When a narrow interval in $s_\parallel$ around the resonance mass is selected, the projection of the data onto $s_\perp$ reflects the angular distribution of the decay products. In vector resonances, a parabolic shape is observed, since the decay width is proportional to cosine squared of the helicity angle, $\cos^2\theta$, where θ is defined as the angle between h_1^- and h_3^+ computed in the (h_1^-, h_2^+) rest frame. If the (h_1^-, h_2^+) pair forms a scalar resonance, the distribution in $s_\perp$ is uniform, since the decay of scalar resonances is isotropic in $\cos\theta$. The interference term between a vector and a scalar resonance is linear in $\cos\theta$.

The CP asymmetry is measured for the following decays: the $B^\pm \to \rho(770)^0 K^\pm$ region and $B^\pm \to \overset{(-)}{K}{}^*(892)^0 \pi^\pm$ from the $B^\pm \to K^\pm \pi^+ \pi^-$ final state; $B^\pm \to \phi(1020)K^\pm$ from $B^\pm \to K^\pm K^+ K^-$ decays; the $B^\pm \to \rho(770)^0\pi^\pm$ region from the $B^\pm \to \pi^\pm \pi^+ \pi^-$ final state; and $B^\pm \to \overset{(-)}{K}{}^*(892)^0 K^\pm$ from $B^\pm \to \pi^\pm K^+ K^-$ decays. It is important to emphasize that the method does not isolate the $\rho(770)^0$ contribution from the influence of the $\omega(782)$ resonance. However, previous analysis show that the fit fractions of amplitudes involving the $\rho(770)^0$ resonances are roughly two orders of magnitude higher than those of the $\omega(782)$ in the $B^\pm \to \rho(770)^0 \pi^\pm$ and $B^\pm \to \rho(770)^0 K^\pm$ decays [21,28]. In addition, their widths are about one order of magnitude different. Therefore, hereafter the P-wave decays in the regions dominated by the $\rho(770)^0$ vector resonance will be denoted as $B^\pm \to \rho(770)^0 \pi^\pm$ and $B^\pm \to \rho(770)^0 K^\pm$.

The method introduced in [12] is described in Sec. IV. A detailed description of the selection, efficiency and background for the four charmless three-body channels is given in a companion paper [29].

II. LHCb DETECTOR AND DATASET

The LHCb detector [30,31] is a single-arm forward spectrometer covering the pseudorapidity range $2 < \eta < 5$, designed for the study of particles containing b or c quarks. The detector includes a high-precision tracking system consisting of a silicon-strip vertex detector surrounding the pp interaction region, a large-area silicon-strip detector located upstream of a dipole magnet with a bending power of about 4 Tm, and three stations of silicon-strip detectors and straw drift tubes placed downstream of the magnet. The tracking system provides a measurement of the momentum, p, of charged particles with a relative uncertainty that varies from 0.5% at low momentum to 1.0% at 200 GeV/c. The minimum distance of a track to a primary pp collision vertex, the impact parameter (IP), is measured with a resolution of $(15 + 29/p_T)$ μm, where p_T is the component of the momentum transverse to the beam, in GeV/c. Different types of charged hadrons are distinguished using information from two ring-imaging Cherenkov detectors. Photons, electrons and hadrons are identified by a calorimeter system consisting of scintillating- pad and preshower detectors, an electromagnetic and a hadronic calorimeter. Muons are identified by a system composed of alternating layers of iron and multiwire proportional chambers.

The online event selection is performed by a trigger, consisting of a hardware stage, based on information from the calorimeter system, followed by a software stage, which applies a full event reconstruction. At the hardware trigger stage, the $B^+ \to h_1^- h_2^+ h_3^+$ candidates are required to include a hadron with transverse energy deposited in the calorimeters typically larger than 3.5 GeV. The software trigger requires a two-, three- or four-track vertex with a significant displacement from all primary vertices. At least one charged particle must have a large transverse momentum and be inconsistent with originating from any primary vertex. A multivariate algorithm is used for the identification of displaced vertices consistent with the decay of a b-hadron.

Simulations are used to model the effects of the detector acceptance and the selection requirements, to validate the fit models and to evaluate efficiencies. In the simulation, pp collisions are generated using PYTHIA 8 [32] with a specific LHCb configuration [33]. Decays of unstable particles are described by EvtGen [34], in which final-state radiation is generated using PHOTOS [35]. The interaction of the generated particles with the detector, and its response, are implemented using the GEANT4 toolkit [36,37] as described in Ref. [38].

III. SELECTION OF SIGNAL CANDIDATES

The selection of signal candidates follows closely the procedure used in the model-independent analysis of the same data sample [39]. Signal B^+ candidates are formed from three tracks that are consistent with originating from

TABLE I. Number of B^+ and B^- candidates in the signal region of 5247 MeV/c^2 to 5315 MeV/c^2 and the corresponding purities.

	$B^\pm \to K^\pm\pi^+\pi^-$	$B^\pm \to K^\pm K^+K^-$	$B^\pm \to \pi^\pm\pi^+\pi^-$	$B^\pm \to \pi^\pm K^+K^-$
B^-	243 960	159 673	51 977	17 161
B^+	240 884	176 345	44 389	21 178
Purity	0.91	0.96	0.88	0.76

the same secondary vertex. Each reconstructed B^+ candidate is associated with the primary vertex that is most consistent with its flight direction. A requirement is also imposed on the angle between the B^+ momentum and the vector between the primary and secondary vertices.

A multivariate analysis is performed to further reduce the combinatorial background. A boosted decision-tree classifier [40] is trained using simulated signal and data in the high-mass sideband region ($m_B > 5.4$ GeV/c^2) for the background. The variables used in this classifier are the quantities based on the quality of the reconstructed tracks and decay vertices, the kinematic properties of the B^+ candidate and its decay products, and the B^+ candidate displacement from the primary vertex. The requirement on the response of this classifier is chosen to optimize the statistical significance of the signal, $\varepsilon_{\text{sim}}/\sqrt{(S+B)_{\text{data}}}$, where ε_{sim} is the signal efficiency determined in simulation and $(S+B)_{\text{data}}$ is obtained by counting the events selected from data within ± 40 MeV/c^2 of the known B^+ mass [41].

Particle identification (PID) is used to reduce the cross-feed from other B decays in which hadrons are incorrectly identified. The main sources of this cross-feed are $K \to \pi$ and $\pi \to K$ misidentification. These backgrounds arising from $K \to \pi$ and $\pi \to K$ misidentification are suppressed by stringent PID requirements for each final-state particle. Tracks that are outside of the fiducial region of the PID system are removed. Furthermore, tracks associated with hits in the muon system are removed to eliminate cross-feed from semileptonic decays.

Candidates within the invariant mass interval 5247–5315 MeV/c^2, which includes approximately 95% of the considered $B^\pm$ decays, are retained for further analysis. The number of $B^\pm$ candidates for each channel used in this analysis, as well as the signal purity, are shown in Table I.

From these candidates, vector resonances are selected by applying restrictions on the $s_\|$ variable around the known mass of each involved resonance, i.e., $\overset{(-)}{K}{}^*(892)^0$, $\rho(770)^0$ and $\phi(1020)$. In the $s_\|$ axis, the data are analyzed in invariant mass intervals of 50, 150 and 5 MeV/c^2,

respectively, centered at the known values of the resonance masses. Since all decay modes have resonances in both $s_\|$ and $s_\perp$, only data with $s_\perp > 5$ GeV^2/c^4 are considered. This requirement ensures that only the interference between scalar and vector resonances in $s_\|$ is relevant. The definition of the interval in $s_\perp$ varies according to the position of the resonance in the phase space. In order to avoid charmonium resonances in the $\pi^+\pi^-$ spectrum of the $B^\pm \to K^\pm\pi^+\pi^-$ decay, an additional veto is applied around the known χ_{c0} and J/ψ invariant masses.

IV. $B \to PV$ FIT FUNCTION

Generally, the decay amplitudes for B^+ and B^- are represented as a coherent sum of intermediate amplitudes, with the magnitude and the phase for each amplitude as free parameters. At low two-body invariant masses the data are dominated by scalar and vector resonances. In the case of one vector resonance interfering with a scalar component, the decay amplitudes can be represented by [12]

$$\mathcal{M}_\pm = a_\pm^V e^{i\delta_\pm^V} F_V^{\text{BW}} \cos\theta(s_\perp, s_\|) + a_\pm^S e^{i\delta_\pm^S} F_S^{\text{BW}}, \quad (1)$$

where $a_\pm^V$ and $a_\pm^S$ are the magnitudes of the vector and scalar resonances, respectively, assumed to be independent of $s_\perp$. $\delta_\pm^V$ and $\delta_\pm^S$ are the phases of the vector and scalar amplitudes, and $\theta(s_\perp, s_\|)$ is the helicity angle. The resonance R may be described by a Breit-Wigner (BW) function, F_R^{BW}, without any loss of generality,

$$F_R^{\text{BW}}(s_\|) = \frac{1}{m_R^2 - s_\| - im_R\Gamma_R(s_\|)}, \quad (2)$$

where $\Gamma_R(s_\|)$ is the energy-dependent relativistic width and m_R is the resonance mass. The helicity angle is a function of the two Dalitz variables, $\cos\theta(s_\|, s_\perp)$ [42]. However, for the low mass and sufficiently narrow resonances, a parabolic dependence of $\cos\theta$ only on $s_\perp$ is a good approximation.

The matrix element squared is

$$\begin{aligned}
|\mathcal{M}_\pm|^2 = {} & (a_\pm^V)^2 (\cos\theta)^2 |F_V^{\text{BW}}|^2 + (a_\pm^S)^2 |F_S^{\text{BW}}|^2 + 2a_\pm^V a_\pm^S \cos\theta |F_V^{\text{BW}}|^2 |F_S^{\text{BW}}|^2 \\
& \times \{\cos(\delta_\pm^V - \delta_\pm^S)[(m_V^2 - s_\|)(m_S^2 - s_\|) + (m_V\Gamma_V)(m_S\Gamma_S)] \\
& + \sin(\delta_\pm^V - \delta_\pm^S)[(m_S\Gamma_S)(m_V^2 - s_\|) - (m_V\Gamma_V)(m_S^2 - s_\|)]\},
\end{aligned} \quad (3)$$

where $m_{V(S)}$ is the vector (scalar) mass and the dependency of $\cos\theta$ on $s_\parallel$ and $s_\perp$ is omitted for simplicity.

Assuming that $a_\pm^V$, $a_\pm^S$ and the phases $\delta_\pm^V$ and $\delta_\pm^S$ do not depend on $s_\perp$, Eq. (3) can be simplified as a quadratic polynomial in $\cos\theta(m_V^2, s_\perp)$ and written as

$$|\mathcal{M}_\pm|^2 = f(\cos\theta(m_V^2, s_\perp)) = p_0^\pm + p_1^\pm \cos\theta(m_V^2, s_\perp) + p_2^\pm \cos^2\theta(m_V^2, s_\perp), \qquad (4)$$

where $p_{0,1,2}^\pm$ are polynomial coefficients. The coefficient $p_0^\pm$ is related to CP violation in the scalar component, whereas $p_1^\pm$ is related to CP violation in the interference between the vector and scalar amplitudes. Since the scalar resonances are usually broad, an amplitude analysis is required to quantify the CP violation in these cases. Given that the decay rates are proportional to $|\mathcal{M}_\pm|^2$, the CP asymmetry A_{CP}^V in the $B \to PV$ decay is given as function of $p_2^\pm$,

$$A_{CP}^V = \frac{|\mathcal{M}_-|^2 - |\mathcal{M}_+|^2}{|\mathcal{M}_-|^2 + |\mathcal{M}_+|^2} = \frac{p_2^- - p_2^+}{p_2^- + p_2^+}. \qquad (5)$$

Given the approximation $\cos\theta(s_\parallel, s_\perp) \simeq \cos\theta(m_V^2, s_\perp)$, $\cos\theta$ becomes a linear function of $s_\perp$ [42]. With this approximation, the CP asymmetry can be obtained from the distribution of $s_\perp$, whereas the asymmetry obtained from the $\cos\theta$ distribution is used to evaluate the systematic uncertainty.

Finally, the function in Eq. (4) is used to fit the histograms of data projected onto the $s_\perp$ axes in order to determine the fit parameters $p_{0,1,2}^\pm$, and then calculate the resulting CP asymmetry using Eq. (5). The asymmetry depends only on the first term of Eq. (3), related to $\cos^2\theta$. The other terms in this equation are constant or linearly dependent on $\cos\theta$.

V. RESULTS

The efficiency-corrected yields of B^+ and B^- as a function of $s_\perp$ are displayed in Fig. 1, with the results of the quadratic fits [Eq. (4)] superimposed. The fit parameters, as well as the corresponding goodness-of-fit parameter χ^2/ndf, are also listed. All asymmetries are computed from the term $p_2^\pm$ and corrected for the B^+-meson production asymmetry [29].

The vector resonances studied in this paper occupy a small part of the charmless three-body B phase-space decay. The combinatorial background behavior in this region is a smooth function of the Dalitz variables, so the parameters $p_0^\pm$ and $p_1^\pm$ absorb it. Another background component is related to the prompt production of these resonances plus a random track. It has an angular distribution similar to the scalar resonances, so it is absorbed in the $p_0^\pm$ parameter.

A. $B^\pm \to \pi^\pm\pi^+\pi^-$ decay

For the $B^+ \to \rho(770)^0\pi^+$ region, the CP asymmetry related to the vector resonance is measured to be

$$A_{CP}(\rho(770)^0\pi^\pm) = -0.004 \pm 0.017,$$

which is compatible with CP symmetry.

The effect of a CP asymmetry compatible with zero can also be seen in Fig. 1(a), which shows the vector parabolas of B^+ and B^- very close to each other. It is important to note that, given the mass window selected, this measurement also includes the $\omega(782)$ contribution.

B. $B^\pm \to K^\pm\pi^+\pi^-$ decay

This decay has two amplitudes involving low-mass vector resonances: $B^\pm \to \overset{(\text{-})}{K}{}^*(892)^0\pi^\pm$ and the region dominated by $B^\pm \to \rho(770)^0K^\pm$ decays. Unlike the result for the $B^+ \to \rho(770)^0\pi^+$ region, the large CP asymmetry obtained here for the $B^+ \to \rho(770)^0K^+$ region can be clearly seen as a difference between the B^+ and B^- parabolas in Fig. 1(b). In this P-wave region dominated by the $\rho(770)^0$ resonance, the CP asymmetry is measured to be

$$A_{CP}(\rho(770)^0K^\pm) = 0.150 \pm 0.019,$$

with a statistical-only significance of 7.9 standard deviations (σ). This measurement can be compared with the values obtained by previous experiments for this channel, as listed in Table II. The results are compatible within the uncertainties.

For $B^+ \to \overset{(\text{-})}{K}{}^*(892)^0\pi^+$ decays, the region with $\pi^+\pi^-$ mass in the range [9, 12] GeV$^2/c^4$ is removed from the fit due to the presence of the J/ψ and χ_{c0} resonances, as can be seen in Fig. 1(c). The CP asymmetry related to the vector resonance is measured to be

$$A_{CP}(\overset{(\text{-})}{K}{}^*(892)^0\pi^\pm) = -0.015 \pm 0.021,$$

which is compatible with CP symmetry.

The exclusion of narrow regions around the charmonium resonances does not affect the sensitivity of the method or the fit quality, since these regions are close to the minimum of the parabolas. Again, the similarity between the B^+ and
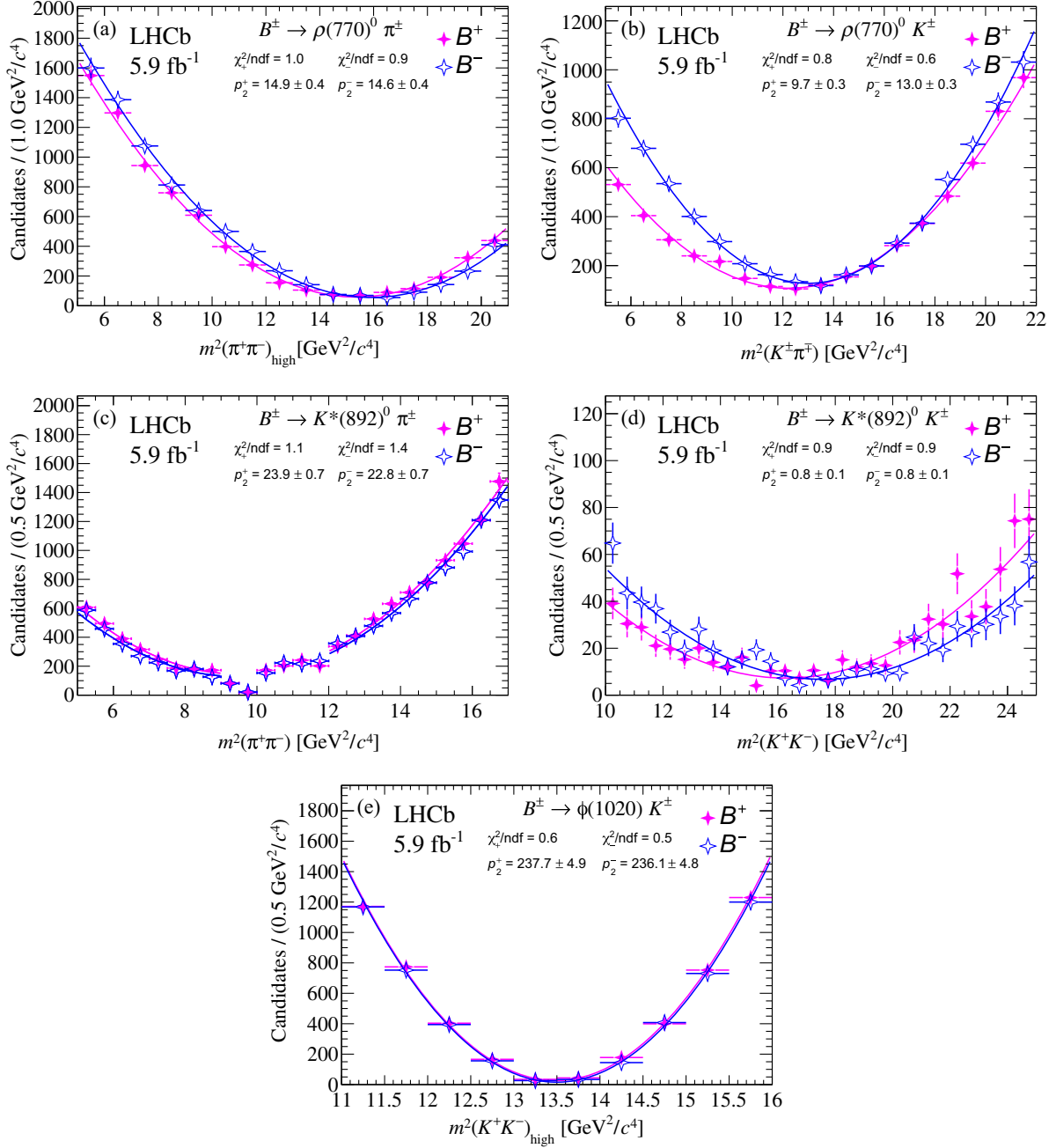
FIG. 1. Distribution of $s_\perp$ for B^+ and B^- candidates and the corresponding quadratic fits for (a) $\rho(770)^0$ in $B^\pm \to \pi^\pm\pi^+\pi^-$, (b) $\rho(770)^0$ in $B^\pm \to K^\pm\pi^+\pi^-$, (c) $\overset{(-)}{K}{}^*(892)^0$ in $B^\pm \to K^\pm\pi^+\pi^-$, (d) $\overset{(-)}{K}{}^*(892)^0$ in $B^\pm \to \pi^\pm K^+K^-$, and (e) $\phi(1020)$ in $B^\pm \to K^\pm K^+K^-$. In the symmetric channels, the phase space distribution and its projections are presented with the two axes being the squares of the low-mass $m_{\rm low}$ and high-mass $m_{\rm high}$ combinations of the opposite-sign particle pairs, for visualization purposes.

B^- parabolas in Fig. 1(c) is compatible with the numerical value obtained.

C. $B^\pm \to \pi^\pm K^+K^-$ decay

For the $B^+ \to \overset{(-)}{K}{}^*(892)^0 K^+$ resonance, the data are analyzed in the range $[10, 25]$ GeV$^2/c^4$, due to the smaller phase space of the $B^\pm \to \pi^\pm K^+K^-$ final state.

The *CP* asymmetry related to the vector resonance, shown in Fig. 1(d), is measured to be

$$A_{CP}(\overset{(-)}{K}{}^*(892)^0 K^\pm) = 0.007 \pm 0.054,$$

which is compatible with *CP* symmetry.

TABLE II. Summary of CP-asymmetry measurements for the vector resonance channels and their associated final-state $B^{\pm} \to R(\to h_1^- h_2^+)h_3^{\pm}$ decays. For comparison purposes, the previous measurements from other experiments are also included.

Decay channel	This work	Previous measurements
$B^{\pm} \to (\rho(770)^0 \to \pi^+\pi^-)\pi^{\pm}$	$-0.004 \pm 0.017 \pm 0.009$	$+0.007 \pm 0.011 \pm 0.016$ (LHCb [20,21])
$B^{\pm} \to (\rho(770)^0 \to \pi^+\pi^-)K^{\pm}$	$+0.150 \pm 0.019 \pm 0.011$	$+0.44 \pm 0.10 \pm 0.04$ (*BABAR* [28]) $+0.30 \pm 0.11 \pm 0.02$ (Belle [22])
$B^{\pm} \to (\overset{(-)}{K}{}^*(892)^0 \to K^{\pm}\pi^{\mp})\pi^{\pm}$	$-0.015 \pm 0.021 \pm 0.012$	$+0.032 \pm 0.052 \pm 0.011$ (*BABAR* [28]) $-0.149 \pm 0.064 \pm 0.020$ (Belle [22])
$B^{\pm} \to (\overset{(-)}{K}{}^*(892)^0 \to K^{\pm}\pi^{\mp})K^{\pm}$	$+0.007 \pm 0.054 \pm 0.032$	$+0.123 \pm 0.087 \pm 0.045$ (LHCb [19])
$B^{\pm} \to (\phi(1020) \to K^+K^-)K^{\pm}$	$+0.004 \pm 0.014 \pm 0.007$	$+0.128 \pm 0.044 \pm 0.013$ (*BABAR* [26])

D. $B^{\pm} \to K^{\pm}K^+K^-$ decay

For $B^+ \to \phi(1020)K^+$ decays, the CP asymmetry related to the vector resonance is measured to be

$$A_{CP}(\phi(1020)K^{\pm}) = 0.004 \pm 0.014,$$

consistent with CP symmetry. This measurement is in agreement with the value obtained by the *BABAR* experiment [26], $A_{CP}(\phi(1020)K^{\pm}) = +0.128 \pm 0.044 \pm 0.013$, at the 2.8σ level. The similarity of the B^+ and B^- distributions in Fig. 1(e) is consistent with the small value of $A_{CP}(\phi(1020)K^{\pm})$ obtained.

VI. SYSTEMATIC UNCERTAINTIES

The three leading sources of systematic uncertainties are discussed below, the dominant one being the variation of the range in $s_{\perp}$ where the fits are performed.

Variation of fit regions: The range in $s_{\perp}$ where the data are fitted varies according to the phase space and the presence of other resonances. The default values of projections, in units of GeV$^2/c^4$, are 5–21 for the $\rho(770)^0$ resonance in $B^{\pm} \to \pi^{\pm}\pi^+\pi^-$ decays, 5–22 for $\rho(770)^0$ in $B^{\pm} \to K^{\pm}\pi^+\pi^-$ decays, 5–17 for $\overset{(-)}{K}{}^*(892)^0$ in $B^{\pm} \to K^{\pm}\pi^+\pi^-$ decay, 10–25 for $\overset{(-)}{K}{}^*(892)^0$ in $B^{\pm} \to \pi^{\pm}K^+K^-$ decay and 11–16 for $\phi(1020)$ in $B^{\pm} \to K^{\pm}K^+K^-$ decay. The intervals are varied by displacing simultaneously both low and high limits by up to 0.5 GeV$^2/c^4$ for $\phi(1020)$ in $B^{\pm} \to K^{\pm}K^+K^-$ decay, and by up to 1 GeV$^2/c^4$ for all other decays.

Variations of resonance mass window: The choice of interval in $s_{\parallel}$ around the resonance mass defines the region where the data are fitted. The intervals in $s_{\parallel}$ are varied around the default values, described in the Sec. III, considering the ranges 140–160 MeV/c^2, 45–55 MeV/c^2 and 4.5–5.5 MeV/c^2 for $\rho(770)^0$, $\overset{(-)}{K}{}^0(892)^0$ and $\phi(1020)$,

respectively. The differences in the results with respect to the default fit are taken as systematic uncertainties in the corresponding CP-asymmetry measurements. The variation is done in small increments, giving 1000 results for each channel. The systematic uncertainties are taken from the root mean square of the resulting asymmetry distributions.

Change of the projected variable: In this case, the fit is performed defining the parabola in terms of the helicity angle $\cos\theta$, instead of $s_{\perp}$. The procedure to obtain the CP asymmetry is the same and the difference with respect to the default fit is taken as systematic uncertainty.

The need for higher-order terms in the fit function is also investigated. These terms would account for a possible influence of $f_2(1270)$ in the $B^{\pm} \to \pi^{\pm}\pi^+\pi^-$ final state. Using simulation [43] and the known value of $\mathcal{B}(f_2(1270) \to \pi^+\pi^-)$, the contribution of the tensor resonance is found to be negligible. Finally, a systematic uncertainty related to the efficiency correction was evaluated and also found to be negligible.

The total systematic uncertainties are obtained as the sum in quadrature of the three contributions. Table II summarizes the results obtained in this analysis.

VII. SUMMARY AND CONCLUSION

In summary, CP asymmetries in charmless $B \to PV$ decays are determined using a new method, without the need for amplitude analyses. The data set analyzed corresponds to an integrated luminosity of 5.9 fb^{-1} of proton-proton collisions collected by the LHCb detector in 2015–2018 at a center-of-mass energy of 13 TeV. Five decay channels are studied, namely $B^{\pm} \to \phi(1020)K^{\pm}$, $B^{\pm} \to \overset{(-)}{K}{}^*(892)^0\pi^{\pm}$, $B^{\pm} \to \rho(770)^0\pi^{\pm}$, $B^{\pm} \to \overset{(-)}{K}{}^*(892)^0K^{\pm}$ and $B^{\pm} \to \rho(770)^0K^{\pm}$. For the $B^{\pm} \to \rho(770)^0K^{\pm}$ region, the CP asymmetry is measured to be $A_{CP} = +0.150 \pm 0.019 \pm 0.011$, which differs from zero by 6.8σ, computed with the total uncertainty.

For the other channels, the measured *CP* asymmetries are compatible with zero, as predicted using the *CPT* constraint [12]. The *CPT* symmetry would suppress *CP* violation in $B \to PV$ decays, which nevertheless could still occur through final-state interactions involving the third particle. A distinct feature of the $B^\pm \to \rho(770)^0 K^\pm$ amplitude in the $B^\pm \to K^\pm \pi^+ \pi^-$ final state is that the contribution from the vector amplitude is much smaller than the scalar contribution, represented by the $B^\pm \to f_0(980)^0 K^\pm$ decay, whereas the opposite is true for the other final states studied.

These measurements are significantly more precise than the previous results obtained by the Belle and *BABAR* Collaborations. Some tension is found between the results of this analysis and those from Belle and *BABAR*, whereas good agreement is found with LHCb results obtained with amplitude analyses of $B^\pm \to \pi^\pm \pi^+ \pi^-$ [20,21] and $B^\pm \to \pi^\pm K^+ K^-$ decays [19].

The method used in this analysis is based on the approximation of a two-body interaction plus one spectator meson, and on the general assumption that the magnitudes and phases of the amplitudes are constant across the whole phase space. These hypotheses, which are assumed by all models used in amplitude analyses, are supported by the quality of the fits.

ACKNOWLEDGMENTS

[1] I. Bediaga and C. Göbel, Direct *CP* violation in beauty and charm hadron decays, Prog. Part. Nucl. Phys. **114**, 103808 (2020).

[2] W. Altmannshofer *et al.* (Belle II Collaboration), The Belle II physics book, Prog. Theor. Exp. Phys. **2019**, 123C01 (2019); **2020**, 029201(E) (2020).

[3] LHCb Collaboration, Physics case for an LHCb upgrade II —Opportunities in flavour physics, and beyond, in the HL-LHC era, arXiv:1808.08865.

[4] M. Beneke, G. Buchalla, M. Neubert, and C. T. Sachrajda, QCD factorization for exclusive, nonleptonic *B* meson decays: General arguments and the case of heavy light final states, Nucl. Phys. **B591**, 313 (2000).

[5] M. Beneke and M. Neubert, QCD factorization for $B \to PP$ and $B \to PV$ decays, Nucl. Phys. **B675**, 333 (2003).

[6] C. Smith, Searching for dominant rescattering sources in *B* to two pseudoscalar decays, Eur. Phys. J. C **33**, 523 (2004).

[7] H.-Y. Cheng, C.-K. Chua, and A. Soni, Effects of final-state interactions on mixing-induced *CP* violation in penguin-dominated *B* decays, Phys. Rev. D **72**, 014006 (2005).

[8] A. R. Williamson and J. Zupan, Two body *B* decays with isosinglet final states in soft collinear effective theory, Phys. Rev. D **74**, 014003 (2006); **74**, 039901(E) (2006).

[9] M. Suzuki, Inelastic final-state interaction, Phys. Rev. D **77**, 054021 (2008).

[10] H.-Y. Cheng, C.-W. Chiang, and A.-L. Kuo, Updating $B \to PP, VP$ decays in the framework of flavor symmetry, Phys. Rev. D **91**, 014011 (2015).

[11] G. Bell, M. Beneke, T. Huber, and X.-Q. Li, Two-loop current–current operator contribution to the non-leptonic QCD penguin amplitude, Phys. Lett. B **750**, 348 (2015).

[12] J. H. Alvarenga Nogueira, I. Bediaga, T. Frederico, P. C. Magalhães, and J. Molina Rodriguez, Suppressed $B \to PV$ *CP* asymmetry: *CPT* constraint, Phys. Rev. D **94**, 054028 (2016).

[13] S.-H. Zhou, Q.-A. Zhang, W.-R. Lyu, and C.-D. Lü, Analysis of charmless two-body *B* decays in factorization-assisted topological-amplitude approach, Eur. Phys. J. C **77**, 125 (2017).

[14] H.-Y. Cheng, *CP* violation in $B^\pm \to \rho^0 \pi^\pm$ and $B^\pm \to \sigma \pi^\pm$ decays, arXiv:2005.06080.

[15] I. Bediaga, I. I. Bigi, A. Gomes, G. Guerrer, J. Miranda, and A. C. dos Reis, On a *CP* anisotropy measurement in the Dalitz plot, Phys. Rev. D **80**, 096006 (2009).

[16] I. I. Bigi, *CP* Asymmetries in many-body final states in beauty & charm transitions, arXiv:1509.03899.

[17] A. Dery, Y. Grossman, S. Schacht, and A. Soffer, Probing the $\Delta U = 0$ rule in three body charm decays, J. High Energy Phys. 05 (2021) 179.

[18] R. Aaij *et al.* (LHCb Collaboration), Amplitude Analysis of the Decay $\bar{B}^0 \to K_S^0 \pi^+ \pi^-$ and First Observation of *CP* Asymmetry in $\bar{B}^0 \to K^*(892)^- \pi^+$, Phys. Rev. Lett. **120**, 261801 (2018).

[19] R. Aaij *et al.* (LHCb Collaboration), Amplitude Analysis of $B^\pm \to \pi^\pm K^+ K^-$ Decays, Phys. Rev. Lett. **123**, 231802 (2019).

[20] R. Aaij *et al.* (LHCb Collaboration), Amplitude analysis of the $B^+ \to \pi^+ \pi^+ \pi^-$ decay, Phys. Rev. D **101**, 012006 (2020).

[21] R. Aaij *et al.* (LHCb Collaboration), Observation of Several Sources of *CP* Violation in $B^+ \to \pi^+ \pi^+ \pi^-$ Decays, Phys. Rev. Lett. **124**, 031801 (2020).

[22] A. Garmash *et al.* (Belle Collaboration), Evidence for Large Direct *CP* Violation in $B^\pm \to \rho(770)^0 K^\pm$ from Analysis of Three-Body Charmless $B^\pm \to K^\pm \pi^\pm \pi^\pm$ Decays, Phys. Rev. Lett. **96**, 251803 (2006).

[23] Y. Nakahama *et al.* (Belle Collaboration), Measurement of *CP* violating asymmetries in $B^0 \to K^+ K^- K_S^0$ decays with a time-dependent Dalitz approach, Phys. Rev. D **82**, 073011 (2010).

[24] B. Aubert *et al.* (*BABAR* Collaboration), An amplitude analysis of the decay $B^\pm \to \pi^\pm \pi^\pm \pi^\mp$, Phys. Rev. D **72**, 052002 (2005).

[25] J. P. Lees *et al.* (*BABAR* Collaboration), Amplitude analysis of $B^0 \to K^+ \pi^- \pi^0$ and evidence of direct *CP* violation in $B \to K^* \pi$ decays, Phys. Rev. D **83**, 112010 (2011).

[26] J. P. Lees *et al.* (*BABAR* Collaboration), Study of *CP* violation in Dalitz-plot analyses of $B^0 \to K^+ K^- K_S^0$, $B^+ \to K^+ K^- K^+$, and $B^+ \to K_S^0 K_S^0 K^+$, Phys. Rev. D **85**, 112010 (2012).

[27] J. P. Lees *et al.* (*BABAR* Collaboration), Evidence for *CP* violation in $B^+ \to K^*(892)^+ \pi^0$ from a Dalitz plot analysis of $B^+ \to K_S^0 \pi^+ \pi^0$ decays, Phys. Rev. D **96**, 072001 (2017).

[28] B. Aubert *et al.* (*BABAR* Collaboration), Evidence for direct *CP* violation from Dalitz-plot analysis of $B^\pm \to K^\pm \pi^\mp \pi^\pm$, Phys. Rev. D **78**, 012004 (2008).

[29] R. Aaij *et al.* (LHCb Collaboration), Direct *CP* violation in charmless three-body decays of $B^\pm$ mesons, Phys. Rev. D **108**, 012008 (2023).

[30] A. A. Alves, Jr. *et al.* (LHCb Collaboration), The LHCb detector at the LHC, J. Instrum. **3**, S08005 (2008).

[31] LHCb Collaboration, LHCb detector performance, Int. J. Mod. Phys. A **30**, 1530022 (2015).

[32] T. Sjöstrand, S. Ask, J. R. Christiansen, R. Corke, N. Desai, P. Ilten, S. Mrenna, S. Prestel, C. O. Rasmussen, and P. Z. Skands, An introduction to PYTHIA 8.2, Comput. Phys. Commun. **191**, 159 (2015).

[33] I. Belyaev *et al.*, Handling of the generation of primary events in Gauss, the LHCb simulation framework, J. Phys. Conf. Ser. **331** (2011) 032047.

[34] D. J. Lange, The EvtGen particle decay simulation package, Nucl. Instrum. Methods Phys. Res., Sect. A **462**, 152 (2001).

[35] N. Davidson, T. Przedzinski, and Z. Was, PHOTOS interface in C++: Technical and physics documentation, Comput. Phys. Commun. **199**, 86 (2016).

[36] S. Agostinelli *et al.* (Geant4 Collaboration), GEANT4: A simulation toolkit, Nucl. Instrum. Methods Phys. Res., Sect. A **506**, 250 (2003).

[37] J. Allison *et al.* (Geant4 Collaboration), GEANT4 developments and applications, IEEE Trans. Nucl. Sci. **53** (2006) 270.

[38] M. Clemencic, G. Corti, S. Easo, C. R. Jones, S. Miglioranzi, M. Pappagallo, and P Robbe, The LHCb simulation application, Gauss: Design, evolution and experience, J. Phys. Conf. Ser. **331**, 032023 (2011).

[39] R. Aaij *et al.* (LHCb Collaboration), Measurement of *CP* violation in the three-body phase space of charmless $B^\pm$ decays, Phys. Rev. D **90**, 112004 (2014).

[40] L. Breiman, J. H. Friedman, R. A. Olshen, and C. J. Stone, *Classification and Regression Trees* (Wadsworth International Group, Belmont, California, USA, 1984).

[41] P. A. Zyla *et al.* (Particle Data Group), Review of particle physics, Prog. Theor. Exp. Phys. **2020**, 083C01 (2020).

[42] E. Byckling and K. Kajantie, *Particle kinematics* (University of Jyvaskyla, Jyvaskyla, Finland, 1971), Chap. I–VI, X.

[43] J. Back *et al.*, LAURA^{++}: A Dalitz plot fitter, Comput. Phys. Commun. **231**, 198 (2018).

R. Aaij,[32] A. S. W. Abdelmotteleb,[50] C. Abellan Beteta,[44] F. Abudinén,[50] T. Ackernley,[54] B. Adeva,[40] M. Adinolfi,[48] H. Afsharnia,[9] C. Agapopoulou,[13] C. A. Aidala,[77] S. Aiola,[25] Z. Ajaltouni,[9] S. Akar,[59] K. Akiba,[32] J. Albrecht,[15] F. Alessio,[42] M. Alexander,[53] A. Alfonso Albero,[39] Z. Aliouche,[56] P. Alvarez Cartelle,[49] S. Amato,[2] J. L. Amey,[48] Y. Amhis,[11] L. An,[42] L. Anderlini,[22] M. Andersson,[44] A. Andreianov,[38] M. Andreotti,[21] D. Ao,[6] F. Archilli,[17] A. Artamonov,[38] M. Artuso,[62] K. Arzymatov,[38] E. Aslanides,[10] M. Atzeni,[44] B. Audurier,[12] S. Bachmann,[17] M. Bachmayer,[43] J. J. Back,[50] A. Bailly-reyre,[13] P. Baladron Rodriguez,[40] V. Balagura,[12] W. Baldini,[21] J. Baptista de Souza Leite,[1] M. Barbetti,[22,j] R. J. Barlow,[56] S. Barsuk,[11] W. Barter,[55] M. Bartolini,[49] F. Baryshnikov,[38] J. M. Basels,[14] G. Bassi,[29,p] B. Batsukh,[4] A. Battig,[15] A. Bay,[43] A. Beck,[50] M. Becker,[15] F. Bedeschi,[29] I. B. Bediaga,[1] A. Beiter,[62] V. Belavin,[38] S. Belin,[27] V. Bellee,[44] K. Belous,[38] I. Belov,[38] I. Belyaev,[38] G. Bencivenni,[23] E. Ben-Haim,[13]

A. Berezhnoy[38] R. Bernet[44] D. Berninghoff,[17] H. C. Bernstein,[62] C. Bertella[56] A. Bertolin[28] C. Betancourt[44] F. Betti,[42] Ia. Bezshyiko[44] S. Bhasin[48] J. Bhom[35] L. Bian[67] M. S. Bieker[15] N. V. Biesuz[21] S. Bifani[47] P. Billoir[13] A. Biolchini[32] M. Birch[55] F. C. R. Bishop[49] A. Bitadze[56] A. Bizzeti, M. Bjørn[57] M. P. Blago[49] T. Blake[50] F. Blanc[43] S. Blusk[62] D. Bobulska[53] J. A. Boelhauve[15] O. Boente Garcia[40] T. Boettcher[59] A. Boldyrev[38] N. Bondar[38,42] S. Borghi[56] M. Borisyak,[38] M. Borsato[17] J. T. Borsuk[35] S. A. Bouchiba[43] T. J. V. Bowcock[54,42] A. Boyer[42] C. Bozzi[21] M. J. Bradley,[55] S. Braun[60] A. Brea Rodriguez[40] J. Brodzicka[35] A. Brossa Gonzalo[50] D. Brundu[27] A. Buonaura[44] L. Buonincontri[28] A. T. Burke[56] C. Burr[42] A. Bursche,[66] A. Butkevich[38] J. S. Butter[32] J. Buytaert[42] W. Byczynski[42] S. Cadeddu[27] H. Cai[67] R. Calabrese[21,i] L. Calefice[15,13] S. Cali[23] R. Calladine[47] M. Calvi[26,m] M. Calvo Gomez[75] P. Camargo Magalhaes[48] P. Campana[23] A. F. Campoverde Quezada[6] S. Capelli[26,m] L. Capriotti[20,g] A. Carbone[20,g] G. Carboni[31] R. Cardinale[24,k] A. Cardini[27] I. Carli[4] P. Carniti[26,m] L. Carus,[14] A. Casais Vidal[40] R. Caspary[17] G. Casse[54] M. Cattaneo[42] G. Cavallero[42] V. Cavallini[21,i] S. Celani[43] J. Cerasoli[10] D. Cervenkov[57] A. J. Chadwick[54] M. G. Chapman,[48] M. Charles[13] Ph. Charpentier[42] C. A. Chavez Barajas[54] M. Chefdeville[8] C. Chen[3] S. Chen[4] A. Chernov[35] V. Chobanova[40] S. Cholak[43] M. Chrzaszcz[35] A. Chubykin[38] V. Chulikov[38] P. Ciambrone[23] M. F. Cicala[50] X. Cid Vidal[40] G. Ciezarek[42] P. E. L. Clarke[52] M. Clemencic[42] H. V. Cliff[49] J. Closier[42] J. L. Cobbledick[56] V. Coco[42] J. A. B. Coelho[11] J. Cogan[10] E. Cogneras[9] L. Cojocariu[37] P. Collins[42] T. Colombo[42] L. Congedo[19,f] A. Contu[27] N. Cooke[47] G. Coombs[53] I. Corredoira[40] G. Corti[42] C. M. Costa Sobral[50] B. Couturier[42] D. C. Craik[58] J. Crkovská[61] M. Cruz Torres[1,e] R. Currie[52] C. L. Da Silva[61] S. Dadabaev[38] L. Dai[65] E. Dall'Occo[15] J. Dalseno[40] C. D'Ambrosio[42] A. Danilina[38] P. d'Argent[42] J. E. Davies[56] A. Davis[56] O. De Aguiar Francisco[56] J. de Boer[42] K. De Bruyn[73] S. De Capua[56] M. De Cian[43] U. De Freitas Carneiro Da Graca[1] E. De Lucia[23] J. M. De Miranda[1] L. De Paula[2] M. De Serio[19,f] D. De Simone[44] P. De Simone[23] F. De Vellis[15] J. A. de Vries[74] C. T. Dean[61] F. Debernardis[19,f] D. Decamp[8] V. Dedu[10] L. Del Buono[13] B. Delaney[49] H.-P. Dembinski[15] V. Denysenko[44] O. Deschamps[9] F. Dettori[27,h] B. Dey[71] A. Di Cicco[23] P. Di Nezza[23] S. Didenko[38] L. Dieste Maronas,[40] H. Dijkstra[42] S. Ding[62] V. Dobishuk[46] C. Dong[3] A. M. Donohoe[18] F. Dordei[27] A. C. dos Reis[1] L. Douglas,[53] A. G. Downes[8] M. W. Dudek[35] L. Dufour[42] V. Duk[72] P. Durante[42] J. M. Durham[61] D. Dutta[56] A. Dziurda[35] A. Dzyuba[38] S. Easo[51] U. Egede[63] V. Egorychev[38] S. Eidelman,[38,†] S. Eisenhardt[52] S. Ek-In[43] L. Eklund[76] S. Ely[62] A. Ene[37] E. Epple[61] S. Escher[14] J. Eschle[44] S. Esen[44] T. Evans[56] L. N. Falcao[1] Y. Fan[6] B. Fang[67] S. Farry[54] D. Fazzini[26,m] M. Feo[42] A. Fernandez Prieto[40] A. D. Fernez[60] F. Ferrari[20] L. Ferreira Lopes[43] F. Ferreira Rodrigues[2] S. Ferreres Sole[32] M. Ferrillo[44] M. Ferro-Luzzi[42] S. Filippov[38] R. A. Fini[19] M. Fiorini[21,i] M. Firlej[34] K. M. Fischer[57] D. S. Fitzgerald[77] C. Fitzpatrick[56] T. Fiutowski[34] F. Fleuret[12] M. Fontana[13] F. Fontanelli[24,k] R. Forty[42] D. Foulds-Holt[49] V. Franco Lima[54] M. Franco Sevilla[60] M. Frank[42] E. Franzoso[21,i] G. Frau[17] C. Frei[42] D. A. Friday[53] J. Fu[6] Q. Fuehring[15] E. Gabriel[32] G. Galati[19,f] A. Gallas Torreira[40] D. Galli[20,g] S. Gambetta[52,42] Y. Gan[3] M. Gandelman[2] P. Gandini[25] Y. Gao[5] M. Garau[27] L. M. Garcia Martin[50] P. Garcia Moreno[39] J. García Pardiñas[26,m] B. Garcia Plana,[40] F. A. Garcia Rosales[12] L. Garrido[39] C. Gaspar[42] R. E. Geertsema[32] D. Gerick,[17] L. L. Gerken[15] E. Gersabeck[56] M. Gersabeck[56] T. Gershon[50] D. Gerstel[10] L. Giambastiani[28] V. Gibson[49] H. K. Giemza[36] A. L. Gilman[57] M. Giovannetti[23,s] A. Gioventù[40] P. Gironella Gironell[39] C. Giugliano[21,i] K. Gizdov[52] E. L. Gkougkousis[42] V. V. Gligorov[13,42] C. Göbel[64] E. Golobardes[75] D. Golubkov[38] A. Golutvin[55,38] A. Gomes[1,a] S. Gomez Fernandez[39] F. Goncalves Abrantes[57] M. Goncerz[35] G. Gong[3] I. V. Gorelov[38] C. Gotti[26] J. P. Grabowski[17] T. Grammatico[13] L. A. Granado Cardoso[42] E. Graugés[39] E. Graverini[43] G. Graziani, A. T. Grecu[37] L. M. Greeven[32] N. A. Grieser[4] L. Grillo[56] S. Gromov[38] B. R. Gruberg Cazon[57] C. Gu[3] M. Guarise[21,i] M. Guittiere[11] P. A. Günther[17] E. Gushchin[38] A. Guth[14] Y. Guz[38] T. Gys[42] T. Hadavizadeh[63] G. Haefeli[43] C. Haen[42] J. Haimberger[42] S. C. Haines[49] T. Halewood-leagas[54] M. M. Halvorsen[42] P. M. Hamilton[60] J. Hammerich[54] Q. Han[7] X. Han[17] E. B. Hansen[56] S. Hansmann-Menzemer[17] L. Hao[6] N. Harnew[57] T. Harrison[54] C. Hasse[42] M. Hatch[42] J. He[6,c] M. Hecker[55] K. Heijhoff[32] K. Heinicke[15] R. D. L. Henderson[63,50] A. M. Hennequin[42] K. Hennessy[54] L. Henry[42] J. Heuel[14] A. Hicheur[2] D. Hill[43] M. Hilton[56] S. E. Hollitt[15] R. Hou[7] Y. Hou[8] J. Hu,[17] J. Hu[66] W. Hu[7] X. Hu[3] W. Huang[6] X. Huang,[67] W. Hulsbergen[32] R. J. Hunter[50] M. Hushchyn[38]

D. Hutchcroft[54] D. Hynds[32] P. Ibis[15] M. Idzik[34] D. Ilin[38] P. Ilten[59] A. Inglessi[38] A. Ishteev[38] K. Ivshin[38] R. Jacobsson[42] H. Jage[14] S. Jakobsen[42] E. Jans[32] B. K. Jashal[41] A. Jawahery[60] V. Jevtic[15] X. Jiang[4,6] M. John[57] D. Johnson[58] C. R. Jones[49] T. P. Jones[50] B. Jost[42] N. Jurik[42] S. Kandybei[45] Y. Kang[3] M. Karacson[42] D. Karpenkov[38] M. Karpov[38] J. W. Kautz[59] F. Keizer[42] D. M. Keller[62] M. Kenzie[50] T. Ketel[33] B. Khanji[15] A. Kharisova[38] S. Kholodenko[38] T. Kirn[14] V. S. Kirsebom[43] O. Kitouni[58] S. Klaver[33] N. Kleijne[29,p] K. Klimaszewski[36] M. R. Kmiec[36] S. Koliiev[46] A. Kondybayeva[38] A. Konoplyannikov[38] P. Kopciewicz[34] R. Kopecna[17] P. Koppenburg[32] M. Korolev[38] I. Kostiuk[32,46] O. Kot,[46] S. Kotriakhova, A. Kozachuk[38] P. Kravchenko[38] L. Kravchuk[38] R. D. Krawczyk[42] M. Kreps[50] S. Kretzschmar[14] P. Krokovny[38] W. Krupa[34] W. Krzemien[36] J. Kubat,[17] W. Kucewicz[35,34] M. Kucharczyk[35] V. Kudryavtsev[38] H. S. Kuindersma,[32] G. J. Kunde[61] T. Kvaratskheliya[38] D. Lacarrere[42] G. Lafferty[56] A. Lai[27] A. Lampis[27] D. Lancierini[44] J. J. Lane[56] R. Lane[48] G. Lanfranchi[23] C. Langenbruch[14] J. Langer[15] O. Lantwin[38] T. Latham[50] F. Lazzari[29,t] M. Lazzaroni[25] R. Le Gac[10] S. H. Lee[77] R. Lefèvre[9] A. Leflat[38] S. Legotin[38] O. Leroy[10] T. Lesiak[35] B. Leverington[17] H. Li[66] P. Li[17] S. Li[7] Y. Li[4] Z. Li[62] X. Liang[62] T. Lin[55] R. Lindner[42] V. Lisovskyi[15] R. Litvinov[27] G. Liu[66] H. Liu[6] Q. Liu[6] S. Liu[4,6] A. Lobo Salvia[39] A. Loi[27] R. Lollini[72] J. Lomba Castro[40] I. Longstaff[53] J. H. Lopes[2] S. López Soliño[40] G. H. Lovell[49] Y. Lu[4,b] C. Lucarelli[22,j] D. Lucchesi[28,n] S. Luchuk[38] M. Lucio Martinez[32] V. Lukashenko[32,46] Y. Luo[3] A. Lupato[56] E. Luppi[21,i] O. Lupton[50] A. Lusiani[29,p] X.-R. Lyu[6] L. Ma[4] R. Ma[6] S. Maccolini[20] F. Machefert[11] F. Maciuc[37] V. Macko[43] P. Mackowiak[15] S. Maddrell-Mander,[48] L. R. Madhan Mohan[48] A. Maevskiy[38] D. Maisuzenko[38] M. W. Majewski,[34] J. J. Malczewski[35] S. Malde[57] B. Malecki[35] A. Malinin[38] T. Maltsev[38] H. Malygina[17] G. Manca[27,h] G. Mancinelli[10] D. Manuzzi[20] C. A. Manzari[44] D. Marangotto[25,l] J. M. Maratas[9,v] J. F. Marchand[8] U. Marconi[20] S. Mariani[22,j] C. Marin Benito[42] M. Marinangeli[43] J. Marks[17] A. M. Marshall[48] P. J. Marshall[54] G. Martelli[72,o] G. Martellotti[30] L. Martinazzoli[42,m] M. Martinelli[26,m] D. Martinez Santos[40] F. Martinez Vidal[41] A. Massafferri[1] M. Materok[14] R. Matev[42] A. Mathad[44] V. Matiunin[38] C. Matteuzzi[26] K. R. Mattioli[77] A. Mauri[32] E. Maurice[12] J. Mauricio[39] M. Mazurek[42] M. McCann[55] L. Mcconnell[18] T. H. McGrath[56] N. T. McHugh[53] A. McNab[56] R. McNulty[18] J. V. Mead[54] B. Meadows[59] G. Meier[15] D. Melnychuk[36] S. Meloni[26,m] M. Merk[32,74] A. Merli[25,l] L. Meyer Garcia[2] M. Mikhasenko[69,d] D. A. Milanes[68] E. Millard,[50] M. Milovanovic,[42] M.-N. Minard,[8,†] A. Minotti[26,m] S. E. Mitchell[52] B. Mitreska[56] D. S. Mitzel[15] A. Mödden[15] R. A. Mohammed[57] R. D. Moise[55] S. Mokhnenko[38] T. Mombächer[40] I. A. Monroy[68] S. Monteil[9] M. Morandin[28] G. Morello[23] M. J. Morello[29,p] J. Moron[34] A. B. Morris[69] A. G. Morris[50] R. Mountain[62] H. Mu[3] F. Muheim[52] M. Mulder[73] K. Müller[44] C. H. Murphy[57] D. Murray[56] R. Murta[55] P. Muzzetto[27] P. Naik[48] T. Nakada[43] R. Nandakumar[51] T. Nanut[42] I. Nasteva[2] M. Needham[52] N. Neri[25,l] S. Neubert[69] N. Neufeld[42] P. Neustroev,[38] R. Newcombe,[55] E. M. Niel[43] S. Nieswand,[14] N. Nikitin[38] N. S. Nolte[58] C. Normand[8] C. Nunez,[77] A. Oblakowska-Mucha[34] V. Obraztsov[38] T. Oeser[14] D. P. O'Hanlon[48] S. Okamura[21,i] R. Oldeman[27,h] F. Oliva[52] M. E. Olivares[62] C. J. G. Onderwater[73] R. H. O'Neil[52] J. M. Otalora Goicochea[2] T. Ovsiannikova[38] P. Owen[44] A. Oyanguren[41] O. Ozcelik[52] K. O. Padeken[69] B. Pagare[50] P. R. Pais[42] T. Pajero[57] A. Palano[19] M. Palutan[23] Y. Pan[56] G. Panshin[38] A. Papanestis[51] M. Pappagallo[19,f] L. L. Pappalardo[21,i] C. Pappenheimer[59] W. Parker[60] C. Parkes[56] B. Passalacqua[21,i] G. Passaleva[22] A. Pastore[19] M. Patel[55] C. Patrignani[20,g] C. J. Pawley[74] A. Pearce[42] A. Pellegrino[32] M. Pepe Altarelli[42] S. Perazzini[20] D. Pereima[38] A. Pereiro Castro[40] P. Perret[9] M. Petric,[53] K. Petridis[48] A. Petrolini[24,k] A. Petrov,[38] S. Petrucci[52] M. Petruzzo[25] H. Pham[62] A. Philippov[38] R. Piandani[6] L. Pica[29,p] M. Piccini[72] B. Pietrzyk[8] G. Pietrzyk[11] M. Pili[57] D. Pinci[30] F. Pisani[42] M. Pizzichemi[26,42,m] V. Placinta[37] J. Plews[47] M. Plo Casasus[40] F. Polci[13,42] M. Poli Lener[23] M. Poliakova[62] A. Poluektov[10] N. Polukhina[38] I. Polyakov[62] E. Polycarpo[2] S. Ponce[42] D. Popov[6,42] S. Popov[38] S. Poslavskii[38] K. Prasanth[35] L. Promberger[42] C. Prouve[40] V. Pugatch[46] V. Puill[11] G. Punzi[29,q] H. R. Qi[3] W. Qian[6] N. Qin[3] R. Quagliani[43] N. V. Raab[18] R. I. Rabadan Trejo[6] B. Rachwal[34] J. H. Rademacker[48] R. Rajagopalan,[62] M. Rama[29] M. Ramos Pernas[50] M. S. Rangel[2] F. Ratnikov[38] G. Raven[33,42] M. Reboud[8] F. Redi[42] F. Reiss[56] C. Remon Alepuz,[41] Z. Ren[3] V. Renaudin[57] P. K. Resmi[10] R. Ribatti[29,p] A. M. Ricci[27] S. Ricciardi[51] K. Rinnert[54] P. Robbe[11] G. Robertson[52] A. B. Rodrigues[43] E. Rodrigues[54] J. A. Rodriguez Lopez[68]

E. Rodriguez Rodriguez,[40] A. Rollings,[57] P. Roloff,[42] V. Romanovskiy,[38] M. Romero Lamas,[40] A. Romero Vidal,[40] J. D. Roth,[77,†] M. Rotondo,[23] M. S. Rudolph,[62] T. Ruf,[42] R. A. Ruiz Fernandez,[40] J. Ruiz Vidal,[41] A. Ryzhikov,[38] J. Ryzka,[34] J. J. Saborido Silva,[40] N. Sagidova,[38] N. Sahoo,[47] B. Saitta,[27,h] M. Salomoni,[42] C. Sanchez Gras,[32] R. Santacesaria,[30] C. Santamarina Rios,[40] M. Santimaria,[23] E. Santovetti,[31,s] D. Saranin,[38] G. Sarpis,[14] M. Sarpis,[69] A. Sarti,[30] C. Satriano,[30,r] A. Satta,[31] M. Saur,[15] D. Savrina,[38] H. Sazak,[9] L. G. Scantlebury Smead,[57] A. Scarabotto,[13] S. Schael,[14] S. Scherl,[54] M. Schiller,[53] H. Schindler,[42] M. Schmelling,[16] B. Schmidt,[42] S. Schmitt,[14] O. Schneider,[43] A. Schopper,[42] M. Schubiger,[32] S. Schulte,[43] M. H. Schune,[11] R. Schwemmer,[42] B. Sciascia,[23,42] A. Sciuccati,[42] S. Sellam,[40] A. Semennikov,[38] M. Senghi Soares,[33] A. Sergi,[24,k] N. Serra,[44] L. Sestini,[28] A. Seuthe,[15] Y. Shang,[5] D. M. Shangase,[77] M. Shapkin,[38] I. Shchemerov,[38] L. Shchutska,[43] T. Shears,[54] L. Shekhtman,[38] Z. Shen,[5] S. Sheng,[4,6] V. Shevchenko,[38] E. B. Shields,[26,m] Y. Shimizu,[11] E. Shmanin,[38] J. D. Shupperd,[62] B. G. Siddi,[21,i] R. Silva Coutinho,[44] G. Simi,[28] S. Simone,[19,f] M. Singla,[63] N. Skidmore,[56] R. Skuza,[17] T. Skwarnicki,[62] M. W. Slater,[47] I. Slazyk,[21,i] J. C. Smallwood,[57] J. G. Smeaton,[49] E. Smith,[44] M. Smith,[55] A. Snoch,[32] L. Soares Lavra,[9] M. D. Sokoloff,[59] F. J. P. Soler,[53] A. Solomin,[38,48] A. Solovev,[38] I. Solovyev,[38] F. L. Souza De Almeida,[2] B. Souza De Paula,[2] B. Spaan,[15,†] E. Spadaro Norella,[25,l] E. Spiridenkov,[38] P. Spradlin,[53] F. Stagni,[42] M. Stahl,[59] S. Stahl,[42] S. Stanislaus,[57] O. Steinkamp,[44] O. Stenyakin,[38] H. Stevens,[15] S. Stone,[62,†] D. Strekalina,[38] F. Suljik,[57] J. Sun,[27] L. Sun,[67] Y. Sun,[60] P. Svihra,[56] P. N. Swallow,[47] K. Swientek,[34] A. Szabelski,[36] T. Szumlak,[34] M. Szymanski,[42] S. Taneja,[56] A. R. Tanner,[48] M. D. Tat,[57] A. Terentev,[38] F. Teubert,[42] E. Thomas,[42] D. J. D. Thompson,[47] K. A. Thomson,[54] H. Tilquin,[55] V. Tisserand,[9] S. T'Jampens,[8] M. Tobin,[4] L. Tomassetti,[21,i] X. Tong,[5] D. Torres Machado,[1] D. Y. Tou,[3] E. Trifonova,[38] S. M. Trilov,[48] C. Trippl,[43] G. Tuci,[6] A. Tully,[43] N. Tuning,[32,42] A. Ukleja,[36,42] D. J. Unverzagt,[17] E. Ursov,[38] A. Usachov,[32] A. Ustyuzhanin,[38] U. Uwer,[17] A. Vagner,[38] V. Vagnoni,[20] A. Valassi,[42] G. Valenti,[20] N. Valls Canudas,[75] M. van Beuzekom,[32] M. Van Dijk,[43] H. Van Hecke,[61] E. van Herwijnen,[38] M. van Veghel,[73] R. Vazquez Gomez,[39] P. Vazquez Regueiro,[40] C. Vázquez Sierra,[42] S. Vecchi,[21] J. J. Velthuis,[48] M. Veltri,[22,u] A. Venkateswaran,[62] M. Veronesi,[32] M. Vesterinen,[50] D. Vieira,[59] M. Vieites Diaz,[43] H. Viemann,[70] X. Vilasis-Cardona,[75] E. Vilella Figueras,[54] A. Villa,[20] P. Vincent,[13] F. C. Volle,[11] D. vom Bruch,[10] A. Vorobyev,[38] V. Vorobyev,[38] N. Voropaev,[38] K. Vos,[74] R. Waldi,[17] J. Walsh,[29] C. Wang,[17] J. Wang,[5] J. Wang,[4] J. Wang,[3] J. Wang,[67] M. Wang,[5] R. Wang,[48] Y. Wang,[7] Z. Wang,[44] Z. Wang,[3] Z. Wang,[6] J. A. Ward,[50,63] N. K. Watson,[47] D. Websdale,[55] C. Weisser,[58] B. D. C. Westhenry,[48] D. J. White,[56] M. Whitehead,[48] A. R. Wiederhold,[50] D. Wiedner,[15] G. Wilkinson,[57] M. K. Wilkinson,[62] I. Williams,[49] M. Williams,[58] M. R. J. Williams,[52] F. F. Wilson,[51] W. Wislicki,[36] M. Witek,[35] L. Witola,[17] G. Wormser,[11] S. A. Wotton,[49] H. Wu,[62] K. Wyllie,[42] Z. Xiang,[6] D. Xiao,[7] Y. Xie,[7] A. Xu,[5] J. Xu,[6] L. Xu,[3] M. Xu,[50] Q. Xu,[6] Z. Xu,[9] Z. Xu,[6] D. Yang,[3] S. Yang,[6] Y. Yang,[6] Z. Yang,[5] Z. Yang,[60] Y. Yao,[62] L. E. Yeomans,[54] H. Yin,[7] J. Yu,[65] X. Yuan,[62] E. Zaffaroni,[43] M. Zavertyaev,[16] M. Zdybal,[35] O. Zenaiev,[42] M. Zeng,[3] D. Zhang,[7] L. Zhang,[3] S. Zhang,[65] S. Zhang,[5] Y. Zhang,[5] Y. Zhang,[57] A. Zharkova,[38] A. Zhelezov,[17] Y. Zheng,[6] T. Zhou,[5] X. Zhou,[6] Y. Zhou,[6] V. Zhovkovska,[11] X. Zhu,[3] X. Zhu,[7] Z. Zhu,[6] V. Zhukov,[14,38] Q. Zou,[4,6] S. Zucchelli,[20,g] D. Zuliani,[28] and G. Zunica[56]

(LHCb Collaboration)

[1]*Centro Brasileiro de Pesquisas Físicas (CBPF), Rio de Janeiro, Brazil*
[2]*Universidade Federal do Rio de Janeiro (UFRJ), Rio de Janeiro, Brazil*
[3]*Center for High Energy Physics, Tsinghua University, Beijing, China*
[4]*Institute of High Energy Physics (IHEP), Beijing, China*
[5]*School of Physics State Key Laboratory of Nuclear Physics and Technology, Peking University, Beijing, China*
[6]*University of Chinese Academy of Sciences, Beijing, China*
[7]*Institute of Particle Physics, Central China Normal University, Wuhan, Hubei, China*
[8]*Université Savoie Mont Blanc, CNRS, IN2P3-LAPP, Annecy, France*
[9]*Université Clermont Auvergne, CNRS/IN2P3, LPC, Clermont-Ferrand, France*
[10]*Aix Marseille Univ, CNRS/IN2P3, CPPM, Marseille, France*

[11]*Université Paris-Saclay, CNRS/IN2P3, IJCLab, Orsay, France*
[12]*Laboratoire Leprince-Ringuet, CNRS/IN2P3, Ecole Polytechnique, Institut Polytechnique de Paris, Palaiseau, France*
[13]*LPNHE, Sorbonne Université, Paris Diderot Sorbonne Paris Cité, CNRS/IN2P3, Paris, France*
[14]*I. Physikalisches Institut, RWTH Aachen University, Aachen, Germany*
[15]*Fakultät Physik, Technische Universität Dortmund, Dortmund, Germany*
[16]*Max-Planck-Institut für Kernphysik (MPIK), Heidelberg, Germany*
[17]*Physikalisches Institut, Ruprecht-Karls-Universität Heidelberg, Heidelberg, Germany*
[18]*School of Physics, University College Dublin, Dublin, Ireland*
[19]*INFN Sezione di Bari, Bari, Italy*
[20]*INFN Sezione di Bologna, Bologna, Italy*
[21]*INFN Sezione di Ferrara, Ferrara, Italy*
[22]*INFN Sezione di Firenze, Firenze, Italy*
[23]*INFN Laboratori Nazionali di Frascati, Frascati, Italy*
[24]*INFN Sezione di Genova, Genova, Italy*
[25]*INFN Sezione di Milano, Milano, Italy*
[26]*INFN Sezione di Milano-Bicocca, Milano, Italy*
[27]*INFN Sezione di Cagliari, Monserrato, Italy*
[28]*Università degli Studi di Padova, Università e INFN, Padova, Padova, Italy*
[29]*INFN Sezione di Pisa, Pisa, Italy*
[30]*INFN Sezione di Roma La Sapienza, Roma, Italy*
[31]*INFN Sezione di Roma Tor Vergata, Roma, Italy*
[32]*Nikhef National Institute for Subatomic Physics, Amsterdam, Netherlands*
[33]*Nikhef National Institute for Subatomic Physics and VU University Amsterdam, Amsterdam, Netherlands*
[34]*AGH—University of Science and Technology, Faculty of Physics and Applied Computer Science, Kraków, Poland*
[35]*Henryk Niewodniczanski Institute of Nuclear Physics Polish Academy of Sciences, Kraków, Poland*
[36]*National Center for Nuclear Research (NCBJ), Warsaw, Poland*
[37]*Horia Hulubei National Institute of Physics and Nuclear Engineering, Bucharest-Magurele, Romania*
[38]*Affiliated with an institute covered by a cooperation agreement with CERN*
[39]*ICCUB, Universitat de Barcelona, Barcelona, Spain*
[40]*Instituto Galego de Física de Altas Enerxías (IGFAE), Universidade de Santiago de Compostela, Santiago de Compostela, Spain*
[41]*Instituto de Fisica Corpuscular, Centro Mixto Universidad de Valencia—CSIC, Valencia, Spain*
[42]*European Organization for Nuclear Research (CERN), Geneva, Switzerland*
[43]*Institute of Physics, Ecole Polytechnique Fédérale de Lausanne (EPFL), Lausanne, Switzerland*
[44]*Physik-Institut, Universität Zürich, Zürich, Switzerland*
[45]*NSC Kharkiv Institute of Physics and Technology (NSC KIPT), Kharkiv, Ukraine*
[46]*Institute for Nuclear Research of the National Academy of Sciences (KINR), Kyiv, Ukraine*
[47]*University of Birmingham, Birmingham, United Kingdom*
[48]*H.H. Wills Physics Laboratory, University of Bristol, Bristol, United Kingdom*
[49]*Cavendish Laboratory, University of Cambridge, Cambridge, United Kingdom*
[50]*Department of Physics, University of Warwick, Coventry, United Kingdom*
[51]*STFC Rutherford Appleton Laboratory, Didcot, United Kingdom*
[52]*School of Physics and Astronomy, University of Edinburgh, Edinburgh, United Kingdom*
[53]*School of Physics and Astronomy, University of Glasgow, Glasgow, United Kingdom*
[54]*Oliver Lodge Laboratory, University of Liverpool, Liverpool, United Kingdom*
[55]*Imperial College London, London, United Kingdom*
[56]*Department of Physics and Astronomy, University of Manchester, Manchester, United Kingdom*
[57]*Department of Physics, University of Oxford, Oxford, United Kingdom*
[58]*Massachusetts Institute of Technology, Cambridge, Massachusetts, USA*
[59]*University of Cincinnati, Cincinnati, Ohio, USA*
[60]*University of Maryland, College Park, Maryland, USA*
[61]*Los Alamos National Laboratory (LANL), Los Alamos, New Mexico, USA*
[62]*Syracuse University, Syracuse, New York, USA*
[63]*School of Physics and Astronomy, Monash University, Melbourne, Australia (associated with Department of Physics, University of Warwick, Coventry, United Kingdom)*
[64]*Pontifícia Universidade Católica do Rio de Janeiro (PUC-Rio), Rio de Janeiro, Brazil (associated with Universidade Federal do Rio de Janeiro (UFRJ), Rio de Janeiro, Brazil)*

[65]*Physics and Micro Electronic College, Hunan University, Changsha City, China (associated with Institute of Particle Physics, Central China Normal University, Wuhan, Hubei, China)*
[66]*Guangdong Provincial Key Laboratory of Nuclear Science, Guangdong-Hong Kong Joint Laboratory of Quantum Matter, Institute of Quantum Matter, South China Normal University, Guangzhou, China (associated with Center for High Energy Physics, Tsinghua University, Beijing, China)*
[67]*School of Physics and Technology, Wuhan University, Wuhan, China (associated with Center for High Energy Physics, Tsinghua University, Beijing, China)*
[68]*Departamento de Fisica, Universidad Nacional de Colombia, Bogota, Colombia (associated with LPNHE, Sorbonne Université, Paris Diderot Sorbonne Paris Cité, CNRS/IN2P3, Paris, France)*
[69]*Universität Bonn—Helmholtz-Institut für Strahlen und Kernphysik, Bonn, Germany (associated with Physikalisches Institut, Ruprecht-Karls-Universität Heidelberg, Heidelberg, Germany)*
[70]*Institut für Physik, Universität Rostock, Rostock, Germany (associated with Physikalisches Institut, Ruprecht-Karls-Universität Heidelberg, Heidelberg, Germany)*
[71]*Eotvos Lorand University, Budapest, Hungary (associated with European Organization for Nuclear Research (CERN), Geneva, Switzerland)*
[72]*INFN Sezione di Perugia, Perugia, Italy (associated with INFN Sezione di Ferrara, Ferrara, Italy)*
[73]*Van Swinderen Institute, University of Groningen, Groningen, Netherlands (associated with Nikhef National Institute for Subatomic Physics, Amsterdam, Netherlands)*
[74]*Universiteit Maastricht, Maastricht, Netherlands (associated with Nikhef National Institute for Subatomic Physics, Amsterdam, Netherlands)*
[75]*DS4DS, La Salle, Universitat Ramon Llull, Barcelona, Spain (associated with ICCUB, Universitat de Barcelona, Barcelona, Spain)*
[76]*Department of Physics and Astronomy, Uppsala University, Uppsala, Sweden (associated with School of Physics and Astronomy, University of Glasgow, Glasgow, United Kingdom)*
[77]*University of Michigan, Ann Arbor, Michigan, USA (associated with Syracuse University, Syracuse, New York, USA)*

[†]Deceased.
[a]Also at Universidade Federal do Triângulo Mineiro (UFTM), Uberaba-MG, Brazil.
[b]Also at Central South University, Changsha, China.
[c]Also at Hangzhou Institute for Advanced Study, UCAS, Hangzhou, China.
[d]Also at Excellence Cluster ORIGINS, Munich, Germany.
[e]Also at Universidad Nacional Autónoma de Honduras, Tegucigalpa, Honduras.
[f]Also at Università di Bari, Bari, Italy.
[g]Also at Università di Bologna, Bologna, Italy.
[h]Also at Università di Cagliari, Cagliari, Italy.
[i]Also at Università di Ferrara, Ferrara, Italy.
[j]Also at Università di Firenze, Firenze, Italy.
[k]Also at Università di Genova, Genova, Italy.
[l]Also at Università degli Studi di Milano, Milano, Italy.
[m]Also at Università di Milano Bicocca, Milano, Italy.
[n]Also at Università di Padova, Padova, Italy.
[o]Also at Università di Perugia, Perugia, Italy.
[p]Also at Scuola Normale Superiore, Pisa, Italy.
[q]Also at Università di Pisa, Pisa, Italy.
[r]Also at Università della Basilicata, Potenza, Italy.
[s]Also at Università di Roma Tor Vergata, Roma, Italy.
[t]Also at Università di Siena, Siena, Italy.
[u]Also at Università di Urbino, Urbino, Italy.
[v]Also at MSU—Iligan Institute of Technology (MSU-IIT), Iligan, Philippines.